

Supporting Information

Saturation dependence of mass transfer for solute transport through residual unsaturated porous media

Zhi Dou^{a,b,*}, Xueyi Zhang^{a,c}, Chao Zhuang^a, Yun Yang^a, Jinguo Wang^a, Zhifang Zhou^a

^a *School of Earth Science and Engineering, Hohai University, Nanjing, 210098 China*

^b *Department of Civil Engineering, University of Toronto, 35 St. George Street, Toronto, ON M5S 1A4, Canada*

^c *Eawag, Swiss Federal Institute of Aquatic Science and Technology, 8600 Dübendorf, Switzerland*

**Corresponding author: Zhi Dou*

E-mail: douz@hhu.edu.cn

1. Direct numerical simulation (DNS) model setup

In this study, both immiscible two-phase transport (ITPT) and Pore-scale aqueous solute transport (PSAST) models were solved by the COMSOL Multiphysics package (COMSOL Inc., Burlington, MA, USA) based on the Galerkin finite-element method. The aqueous and non-aqueous phase liquids were assumed as water and Trichloroethylene (TCE), respectively. The density of water and TCE at 293.15K were 998.2 kg/m^3 and 1460 kg/m^3 , respectively. The wetting angle was $\theta = \pi/6$. The interfacial tension between water and TCE were $\sigma=36.9 \text{ mN/m}$ [1]. The viscosity of water and TCE were $\mu_w = 1.002 \times 10^{-3} \text{ kg/(m} \cdot \text{s)}$ and $\mu_{nw}=5.3 \times 10^{-4} \text{ kg/(m} \cdot \text{s)}$ at 293.15K, respectively. The molecular diffusion coefficient of conservative aqueous tracer was set to be $D_m=1.0 \times 10^{-9} \text{ m}^2/\text{s}$.

1.1 ITPT model

The porous media was initially saturated by TCE. The left and right boundaries of porous media were inlet and outlet boundaries, respectively. The water was injected along the inlet boundary with three specific flow rates (e.g., $u=0.60, 0.15$, and 0.05 m/s). The corresponding capillary numbers were $\log Ca=-4.12, -5.50$, and -6.60 , while the viscosity ratio was constant and equal to $M=\mu_w/\mu_{nw}=1.89$. The outlet boundary was set as zero pressure boundary condition. The non-slip

boundary was applied on the immiscible interfaces between TCE, water and soil.

Solving the ITP model by the COMSOL Multiphysics package, the backward differentiation formula (BDF) was employed to automatically adjust the time step. The time dependent solver (PARDISO) was selected as system solver. The Phase Field Method module and Laminar flow module were coupled and solved in the ITP model. The Phase Field Multiphysics coupling feature defines the density and dynamic viscosity of the fluid used in the Laminar Flow interfaces. It defines the surface tension on the interface in the form of a volume force used in the momentum equation. It also allows the Phase Field interface to use the velocity field calculated from the Laminar Flow interface. For ITP model, the mobility tuning parameter χ and the thickness of the interface between the two immiscible fluids ε were significant for the reality and accuracy of solutions [2], since the value of χ must be high enough to keep the interface thickness constant and low enough not to damp the advection. Depending on previous study [3], in this study, the mobility tuning parameter χ and the thickness of the interface between the two immiscible fluids ε were set as $\chi=1$ and $\varepsilon=h_{max}/6$ where the h_{max} represents the maximum mesh size. The computational domain for ITP model in the porous medium was discretized into 86225 triangular elements. The mesh size was set to a range from 2.7×10^{-3} mm to $2.34 \times$

10^{-1} mm. The mesh independence analysis was conducted to ensure numerical stability and accuracy. Under the same boundary condition, three different meshes with different triangular elements (e.g., $M_n = 19616$, 86225, and 127628) were tested. As shown in Fig S1, TCE saturation was independent on mesh when the M_n was more than 86225, indicating that the 86225 triangular elements were enough to provide stable and accurate numerical results. Therefore, 86225 triangular elements were used in this study.

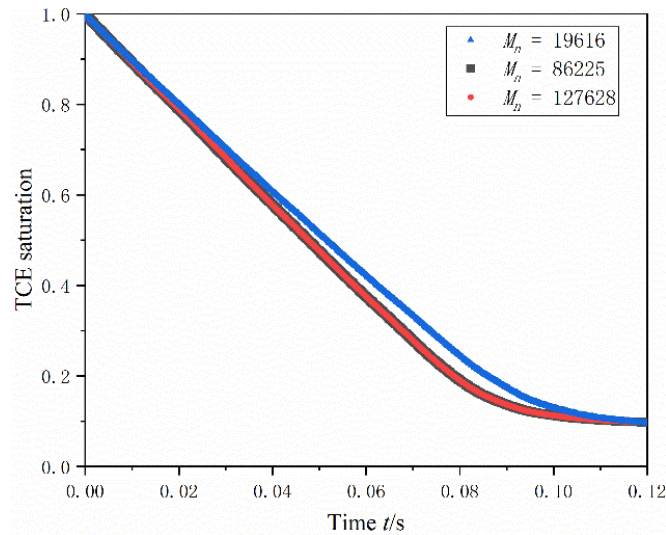


Fig S1 TCE saturation dependence of mesh

1.2 PSAST model

After obtaining residual TCE distribution by the ITPT model in porous media, the PSAST model was implemented on the pore space occupied by water. For the flow field in the PSAST model, the boundary conditions were set as follows: the left and right boundaries were set to be the first-type boundary as inlet and outlet boundaries, respectively. The steady

flow was driven from left to right by the given pressure gradient (i.e., $-\nabla p = 122 \text{ Pa/m}$) for all of flow field in the aqueous phase. The no-slip boundary condition was applied at the solid-liquid and liquid-liquid interfaces. There was no flux across the top and bottom boundaries. For the aqueous solute transport, the pore space was initially occupied by water and there was no tracer in the aqueous pore space. The pulsed tracer with the concentration c_0 was injected along the inlet boundary. The step function was used to simulate the pulsed injection condition. The inlet and outlet boundary conditions for the aqueous solute transport were specified as,

$$c(0, t) = \begin{cases} c_0, & 0 < t \leq 2t' \\ 0, & 2t' < t \end{cases} \quad (1)$$

$$\partial c(L, t) / \partial n = 0 \quad t \geq 0 \quad (2)$$

where L is the length of porous media geometry, n represents the direction normal to the outlet boundary, and t' is the dimensionless time or so-called pore volume Pv . The Pv was defined as,

$$Pv = \frac{Qt}{V_w} \quad (3)$$

where Q is the flow rate (L^3T^{-1}), V_w represents the volume of pore space occupied by aqueous liquid (L^3). Since the conservative and non-reactive tracer was introduced, the no-slip boundary condition was

applied at the solid-liquid and liquid-liquid interfaces. The BTCs were obtained by the ratio of effluent solute mass to fluid mass,

$$c_f = \frac{\int_0^h \bar{u} c dz}{\int_0^h \bar{u} dz} \quad (4)$$

1.3 Validation of numerical model

Two benchmark cases are provided here to validate our numerical model. The results of validation cases agree very well with the results of previous study or theoretical results, which validates the correctness of numerical models.

ITPT model

We simulated the process of two-dimensional bubbles rising in liquid columns due to the buoyancy force and compared it with the results of Hysing et al [4]. The mass center and rising velocity of the bubble at different times are calculated respectively, as shown in Fig S2. The simulation results agree quite well with the results of Hysing et al., which validates the correctness of numerical models.

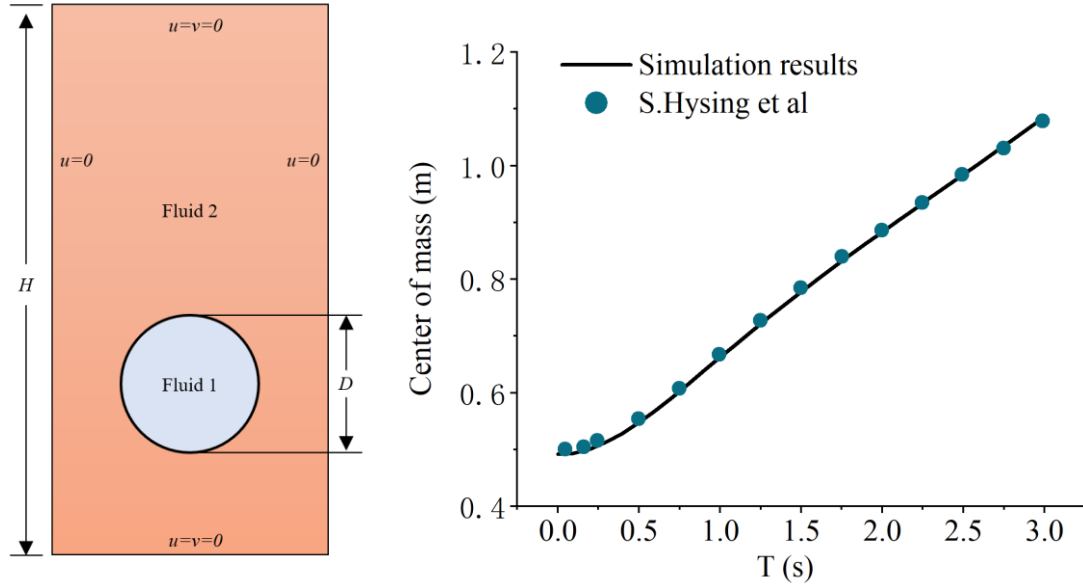


Figure S2 Initial configuration and boundary conditions of the bubble rising case (a). Time evolution of the mass center (b).

PSAST model

We simulated the solute transport process in a parallel plate and calculated the Taylor dispersion coefficient (D_{taylor}). Taylor dispersion is an effect in fluid mechanics in which a shear flow can increase the effective diffusivity of a species[5]. The seminal Taylor's work [6] demonstrates that for solute transport through parallel plates where the fluid follows the stratified flow, the effective solute transport eventually becomes one dimensional and the shear-flow-induced dispersion can be measured by an effective longitudinal dispersion (i.e. Taylor dispersion) and mean flow velocity \bar{u} . The Taylor dispersion coefficient for an ideal 2D paralleled fracture is given as,

126

$$D_{Taylor} = \frac{\bar{u}^2 \bar{b}^2}{210 D_m} \quad (5)$$

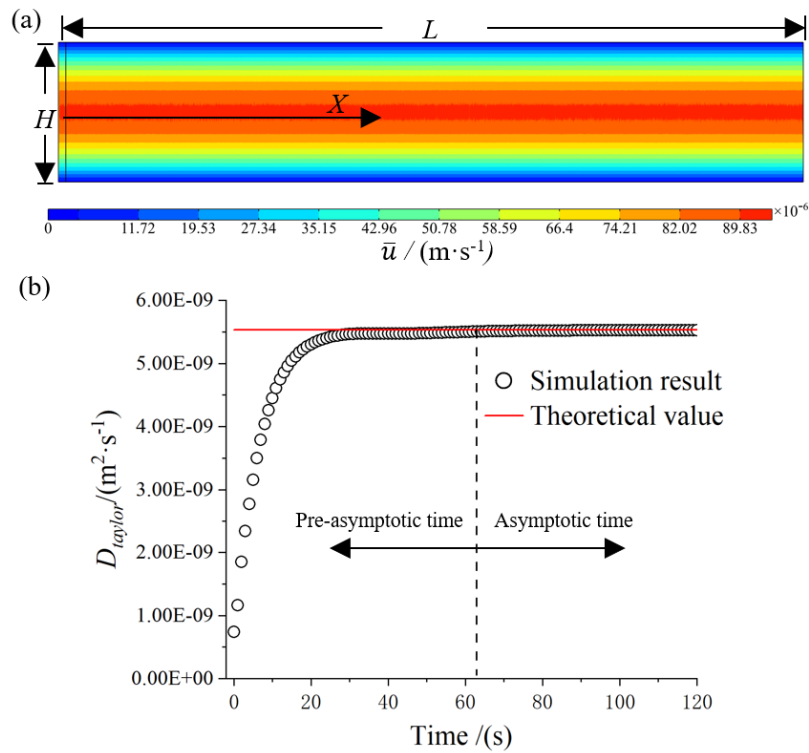
127

128

129

130

In this case, the length and height of the parallel plate was $L=200$ mm and $H=0.5$ mm, the ratio of length to height is $L/H=400$, and the corresponding asymptotic time is $\tau = b^2/4D_m = 62.5$ s. The average flow velocity in the fracture is $\bar{u} = 6.17 \times 10^{-5}$ m/s.



131

132

133

Fig S3. The shear flow in a parallel plate (a). The dynamic variation process of Taylor dispersion coefficient

134

135

136

As shown in Fig S3, before the progressive time, the dispersion coefficient is not a fixed value, but a function related to time. According to the physical meaning of spatial moment, the dispersion coefficient in X

direction can be expressed by the change rate of second-order moment in X direction,

$$2D_x = \lim_{t \rightarrow \infty} \frac{dM_{2,xx}}{dt} \quad (6)$$

The total mass of solute in the calculation area is calculated by using the spatial moment of solute cluster

$$M = \int_{\Omega} C(x, t) d\Omega \quad (7)$$

First moment in X direction:

$$M_{1,x}(t) = \int_{\Omega} C(x, t) x d\Omega \quad (8)$$

Second moment in X direction:

$$M_{2,xx}(t) = \frac{\int_{\Omega} C(x, t) (x - M_{1,x}/M)(x - M_{1,x}/M) d\Omega}{M} \quad (9)$$

It can be seen from Fig.S3 that the dispersion coefficient increases with time before the progressive time; Near the asymptotic time, the dispersion coefficient calculated by the second-order moment in the X direction is close to the theoretical value of Taylor dispersion coefficient.

2. Definition of Peclet number and Reynolds number

The Peclet number is defined by $Pe = \tau_D/\tau_a = 2\bar{r}\bar{u}/D_m$. It is the ratio of the characteristic diffusion time $\tau_D = 2\bar{r}\bar{u}/D_m$ to the characteristic advection time $\tau_a = \bar{u}/2\bar{r}$. The fixed pressure gradient between inlet

and outlet boundaries was applied in all cases, result in the Pe range from 393.87 to 286.96.

The Reynold number was defined by $Re = 2\bar{r}\rho\bar{u}/\mu$. It is commonly used to predict the onset of non-Darcy flow and to determine the flow regime. In this study, the Re range from 0.39 to 0.29, indicating that the flow was Darcy regime for all cases.

3. Inverse model for aqueous tracer transport

3.1 Advection dispersion equation (ADE) model

The classical Advection Dispersion Equation (ADE), which based on Fick's law, was used to fit the BTCs for all cases. The 1D governing equation of ADE model is given by

$$\frac{\partial c}{\partial t} = -\nabla \cdot (\overline{u_{ADE}} c) + D_{ADE} \nabla^2 c \quad (10)$$

Where the D_{ADE} is the fitted dispersion coefficient and $\overline{u_{ADE}}$ is the mean flow velocity. We used the STANMOD V2.08 software[7] for the inverse calculations.

The initial estimated value of $\overline{u_{ADE}}$ was set to the \bar{u} obtained by direct simulation. In this study, the tracer pulse with concentration c_0 was injected into porous media for $2\text{ }Pv$ at the inlet boundary. Therefore, in STANMOD, we used the pulse input at application time boundary condition. The input concentration was set to the dimensionless

concentration. The corresponding application times were 162.8, 152.9, 223.2, and 250.4 s, respectively. For each case, total 150 data points from BTC were used for the inverse calculations.

3.2 Continuous time random walk (CTRW) model

The CTRW transport equation is generally based on the Fokker-Planck with memory equation (FPME) which originally describes the temporal evolution of the probability density function of the velocity of a particle under the influence of drag forces and random forces. In CTRW, the Laplace transformed concentration function

$$p\bar{c}(x, p) - c_0(x) = -\bar{M}(p) \left[\overline{u_{ctrw}} \frac{\partial \bar{c}(x, p)}{\partial x} - D_{ctrw} \frac{\partial^2 \bar{c}(x, p)}{\partial x^2} \right] \quad (11)$$

where p is the Laplace variable, $\overline{u_{ctrw}}$ and D_{ctrw} are mean flow velocity and fitted dispersion coefficient in the framework of CTRW, respectively. In Eq. (11), the memory function $\bar{M}(p)$ captures the anomalous or non-Fickian transport induced by local heterogeneity or process and the corresponding formulation is given by

$$\bar{M}(p) = -\bar{t}p \frac{\bar{\psi}(p)}{1 - \bar{\psi}(p)} \quad (12)$$

where \bar{t} is some characteristic time and $\bar{\psi}(p)$ is the transition rate probability which is the core of the CTRW model. In this study, we used the truncated power law (TPL) for $\bar{\psi}(p)$. The TPL model is given by

$$\psi(p) = \frac{(1 + \tau_2 p t_1)^{\beta_{CTRW}} \exp(t_1 p) \Gamma(-\beta_{CTRW}, \tau_2^{-1} + t_1 p)}{\Gamma(-\beta_{CTRW}, \tau_2^{-1})} \quad (13)$$

where t_l represents the lower limit time when the power law behavior begins, $\tau_2 = t_2/t_1$, t_2 is the cut-off time describing the Fickian behavior dominates, $\Gamma()$ represents the incomplete Gamma function, and the parameter β_{CTRW} indicates the different types of anomalous transport.

In this study, the CTRW Matlab Toolbox V4.0 [8] was employed for the inverse calculations. For the inverse model using the CTRW TPL, there were five initial input parameters, t_l , t_2 , $\overline{u_{ctrw}}$, β_{CTRW} and D_{ctrw} . The initial estimate for the velocity $\overline{u_{ctrw}}$ and dispersion D_{ctrw} were assumed to be equal to the values from the ADE inverse modeling. Note that the input value of $\overline{u_{ctrw}}$ and D_{ctrw} need to be in units of 1/time. We divided the $\overline{u_{ctrw}}$ and D_{ctrw} by the L (length of the porous media, $L=0.041\text{m}$) and L^2 . The initial estimate for t_l , t_2 , and β_{CTRW} were set to be 10^{-2} , 10^3 , and 1.8, respectively.

Reference

- [1] M.P. Andersson, M.V. Bennetzen, A. Klamt, S.L.S. Stipp, First-Principles Prediction of Liquid/Liquid Interfacial Tension, *Journal of Chemical Theory and Computation*, 10(8) (2014) 3401–3408.

- 216 [2] D. Jacqmin, Calculation of Two-Phase Navier - Stokes Flows Using Phase-
 217 Field Modeling, *Journal of Computational Physics*, 155(1) (1999) 96-127.
- 218 [3] G. Zhu, J. Yao, A. Li, H. Sun, L. Zhang, Pore-Scale Investigation of
 219 Carbon Dioxide-Enhanced Oil Recovery, *Energy & Fuels*, 31(5) (2017) 5324-
 220 5332.
- 221 [4] S. Hysing, S. Turek, D. Kuzmin, N. Parolini, E. Burman, S. Ganesan, L.
 222 Tobiska, Quantitative benchmark computations of two-dimensional bubble
 223 dynamics, *International Journal for Numerical Methods in Fluids*, 60(11)
 224 (2009) 1259-1288.
- 225 [5] G.I. Taylor, Dispersion of soluble matter in solvent flowing slowly
 226 through a tube, *Proceedings of the Royal Society of London. Series A.*
 227 *Mathematical and Physical Sciences*, 219(1137) (1953) 186-203.
- 228 [6] R. Aris, On the Dispersion of a Solute in a Fluid Flowing through a
 229 Tube, *Proceedings of the Royal Society of London A: Mathematical, Physical*
 230 *and Engineering Sciences*, 235(1200) (1956) 67-77.
- 231 [7] N. Toride, F. Leij, M.T. Van Genuchten, The CXTFIT code for estimating
 232 transport parameters from laboratory or field tracer experiments, US
 233 Salinity Laboratory Riverside, CA, 1995.
- 234 [8] A. Cortis, B. Berkowitz, Computing “Anomalous” Contaminant Transport
 235 in Porous Media: The CTRW MATLAB Toolbox, *Groundwater*, 43(6) (2005) 947-
 236 950.

237